



Cite this: *Org. Biomol. Chem.*, 2016, **14**, 701

Molecular construction of HIV-gp120 discontinuous epitope mimics by assembly of cyclic peptides on an orthogonal alkyne functionalized TAC-scaffold†

P. R. Werkhoven,^a M. Elwakiel,^a T. J. Meuleman,^a H. C. Quarles van Ufford,^a J. A. W. Kruijtzter^a and R. M. J. Liskamp^{*a,b}

Mimics of discontinuous epitopes of for example bacterial or viral proteins may have considerable potential for the development of synthetic vaccines, especially if conserved epitopes can be mimicked. However, due to the structural complexity and size of discontinuous epitopes molecular construction of these mimics remains challenging. We present here a convergent route for the assembly of discontinuous epitope mimics by successive azide alkyne cycloaddition on an orthogonal alkyne functionalized scaffold. Here the synthesis of mimics of the HIV gp120 discontinuous epitope that interacts with the CD4 receptor is described. The resulting protein mimics are capable of inhibition of the gp120–CD4 interaction. The route is convergent, robust and should be applicable to other discontinuous epitopes.

Received 27th September 2015,
Accepted 5th November 2015

DOI: 10.1039/c5ob02014j

www.rsc.org/obc

Introduction

There is great therapeutic potential for protein surface mimics of bacterial and viral proteins involved in infectious diseases. These protein mimics may be capable of inhibition or even prevention of the binding of these proteins to their cellular targets and are important for the design of synthetic vaccines.

As part of a program to address the synthetic challenges for the construction of protein mimics encompassing different peptide segments, we have been involved in (1) the development of syntheses of different scaffolds for the attachment of (cyclic) peptides,¹ (2) synthetic approaches for the attachment of different (cyclic) peptides to these scaffolds² and (3) the generation of libraries of the resulting protein mimics.³

The practicality and efficiency of the synthesis of protein mimics, with respect to yield, purity and possibilities for expansion to collections or libraries, is an increasingly important issue in the preparation of these relatively complex biomolecular constructs of “intermediate size”.⁴ Convergent methods for introducing both different and several peptide loops onto suitable scaffolds would greatly contribute to this.

Synthesis of especially discontinuous epitope mimics remains very challenging because of their structural complexity. A continuous epitope, which consists of a single contiguous row of amino acids (Fig. 1 left), can be relatively easily mimicked by one corresponding single linear or cyclic peptide. In contrast to this, mimicry of a discontinuous epitope, which consists of multiple peptide segments of the protein that are far apart in the primary sequence but are brought together by the folding of the protein (Fig. 1 right), is far more challenging.

Our strategy for the mimicry of discontinuous epitopes is scaffolding (Fig. 2). In this approach peptides corresponding to the amino acid sequence of the epitope are synthesized and attached to a small molecular scaffold. This scaffold should provide the pre-organization of the peptides that is required to accurately mimic an epitope. Many current synthetic routes for

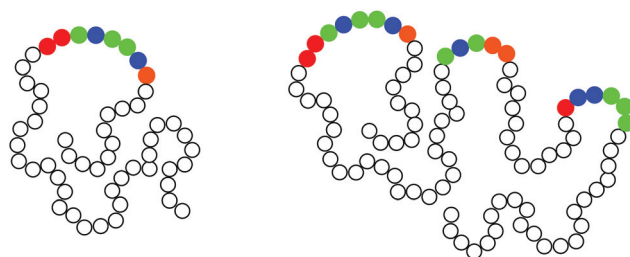


Fig. 1 Structural classes of protein–protein interaction sites: continuous (left) and discontinuous (right).

^aDivision of Medicinal Chemistry & Chemical Biology, Department of Pharmaceutical Sciences, Faculty of Science, Utrecht University, PO Box 80082, 3508 TB Utrecht, The Netherlands. E-mail: r.m.j.liskamp@uu.nl

^bSchool of Chemistry, Joseph Black Building, University of Glasgow, University Avenue, Glasgow, G12 8QQ, UK. E-mail: robert.liskamp@glasgow.ac.uk

†Electronic supplementary information (ESI) available: Analytical data for peptides, constructs and intermediates. See DOI: 10.1039/c5ob02014j



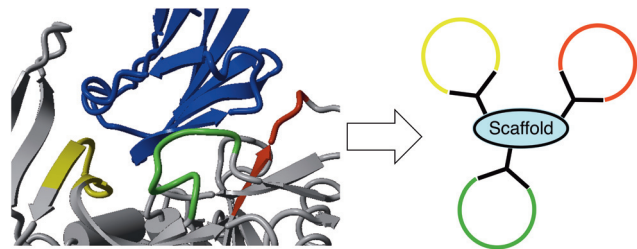


Fig. 2 The CD4-binding site of HIV-gp120 (gray) in complex with CD4 (blue).⁷ Peptides corresponding to the parts of the protein that are responsible for binding (yellow, green and red) can be mounted onto a molecular scaffold to create a mimic of the interaction sites.

a scaffolded protein mimic are often lengthy and not very efficient.^{2a,b,5} Furthermore, most synthetic routes are developed for incorporation of linear peptides or do not allow for the introduction of different peptides.^{2b,3a,b,6} It is believed that cyclic peptides provide better mimics of the shape of the epitope as it is in the protein context. An additional, albeit very important reason for incorporation of cyclic peptides is the possible increased proteolytic stability, which from a therapeutic applications perspective is a determining factor.

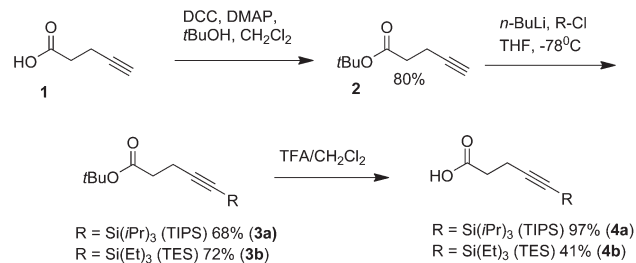
Recently, we described a convergent synthesis of protein mimics by sequential native chemical ligation.^{2d} Here, we describe a more robust convergent synthetic route for the assembly of three cyclized peptides to an orthogonal alkyne functionalized scaffold. The versatile preparation of the scaffold and the convenient accessibility of the cyclic peptides are clear indicators of this robustness. Our synthesis strategy is illustrated by the synthesis of protein mimics of the viral envelope HIV gp120 protein encompassing its binding site with CD4 cellular receptor (Fig. 2). The resulting mimics are able to compete with gp120 for binding to CD4 in an ELISA assay.

In contrast to our earlier work,⁸ we have streamlined the synthesis of the required scaffold. In addition, the sequential ligation procedure has been improved by combining the cyclization and deprotection reactions in a single pot. Finally, it is shown that the synthesized mimics are capable of behaving as a protein mimic of HIV gp120 interacting with the CD4 receptor.

Results and discussion

Scaffold synthesis

Introduction of the (protected) alkynes moieties was achieved using (protected) pentynoic acid derivatives. The choice of the triethylsilyl (TES) and triisopropylsilyl (TIPS) groups was originally based on the work of Valverde *et al.*⁹ Our previous results have shown that this strategy worked excellently.⁸ The synthesis of protected pentynoic acid derivatives is shown in Scheme 1. First, the carboxylic acid functionality of pentynoic acid (**1**) was protected as a *tert*-butyl ester (**2**). Next, the silyl-



Scheme 1 Synthesis of silyl-protected pentynoic acid derivatives.

protecting groups were introduced using *n*-BuLi and triethylsilyl chloride or triisopropylsilyl chloride. Both protected alkynes (**3a** & **3b**) were obtained in good yields (*ca.* 70%). By treatment with TFA the *t*Bu ester was hydrolysed to afford the final silyl protected pentynoic acid derivatives (**4a** and **4b**). From the modest yield of the TES-protected derivative (41%) it is apparent that the TES-group is less stable under these conditions and because of this the TES-protected pentynoic acid was introduced near the end of the synthesis of the alkyne functionalized scaffold. The synthesis of the scaffold could be streamlined by adaptation and expansion of our earlier work (Scheme 2).¹⁰ Starting from 3-bromopropylamine hydrobromide (**5**), the first step was the introduction of the *o*NBS protecting group to afford *o*NBS-protected bromopropaneamine (**6**) in an excellent yield (96%). Next, triamine **7** was prepared by reaction with 1,3-diaminopropane in DMA, followed by the protection of the other primary amine of triamine **7** with a trifluoroacetyl (TFA) protection group, using ethyl trifluoroacetate. Coupling of pentynoic acid to the secondary amine using BOP afforded triamine **9** in a yield of 67% over 3 steps.

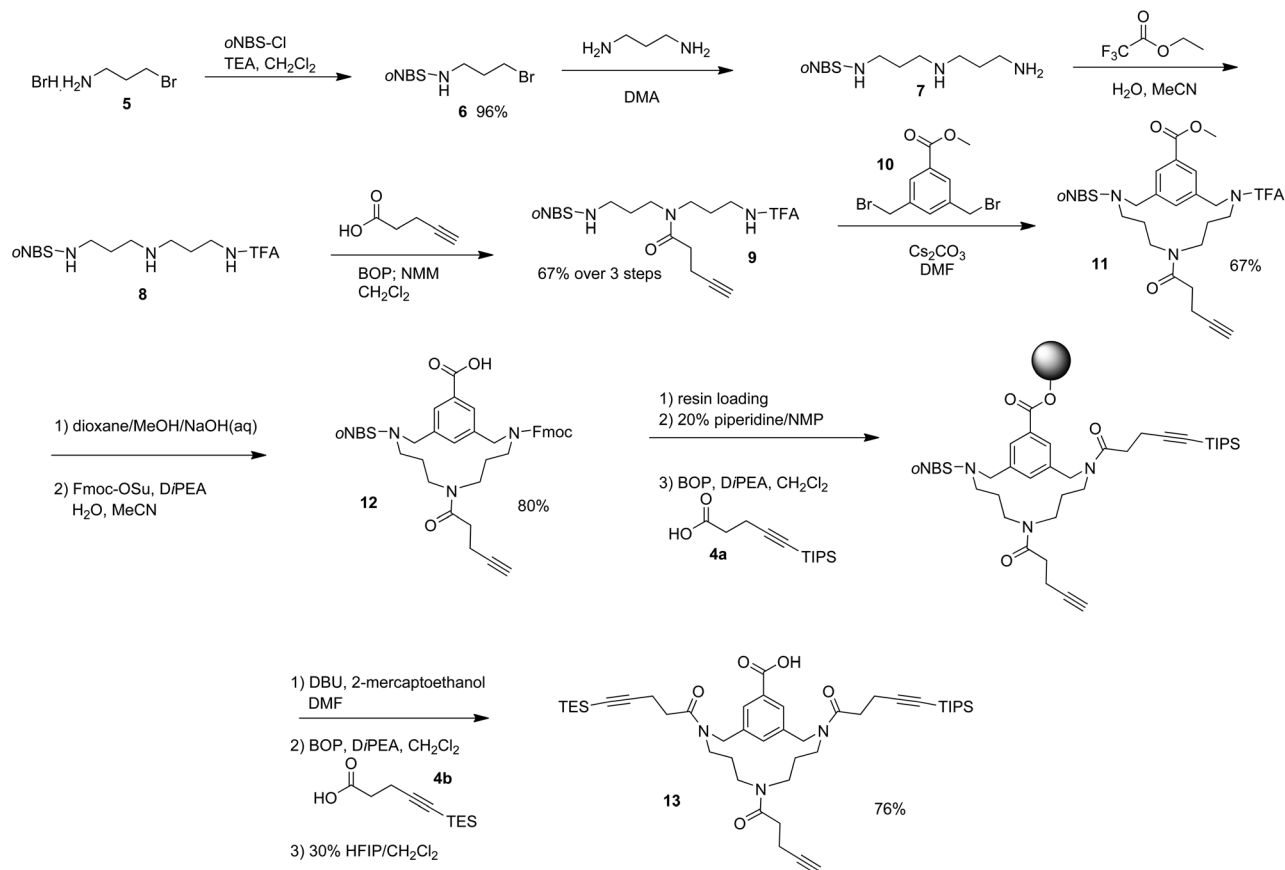
Cyclization of the triamine was achieved by reaction with dibromide **10**, which was easily synthesized following a literature procedure,¹¹ to give the skeleton of the TAC-scaffold (**11**) in 67% yield. Treatment with base removed the methylester and trifluoroacetyl protecting group. This was followed by protection of the now free amine with an Fmoc-group to give the desired free carboxylic acid TAC (**12**) in an 80% yield.

The Fmoc- and *o*NBS protected scaffold (**12**) was then loaded on 2-chlorotriyl-chloride resin. The Fmoc-group was removed by treatment with piperidine, followed by the BOP-coupling of TIPS-protected pentynoic acid (**4a**). Next, the *o*NBS-group was removed, followed by the coupling of TES-protected pentynoic acid (**4b**). Cleavage from the resin with HFIP resulted in the final protected trialkyne scaffold (**13**) in a good overall yield (76% over 6 steps).

Peptide synthesis

Cyclic peptides were synthesized using the method that we previously described (Fig. 3).⁸ This method was inspired by the work of Timmerman *et al.*¹² in which terminal cysteine residues were alkylated with benzylic dibromide derivative to cyclize the peptide. In our approach the dibromide was also





Scheme 2 Synthesis of the protected tri-alkyne scaffold. The synthesis is an adaptation and expansion on the most recent synthesis of the orthogonally protected triamine TAC-scaffold.¹⁰

outfitted with a benzylic azide (**13**) for the attachment to the scaffold. To investigate the influence of peptide cyclization, linear peptides were also prepared. For the synthesis of the linear peptides only one cysteine was present in the peptide. This cysteine residue was alkylated with an azide-containing mono-bromide (**14**). Using this method we synthesized peptides involved in the binding of gp120 to the CD4 receptor (Fig. 3). Due to a poor solubility of peptide **17** it was not acetylated on the N-terminus to improve its solubility. Therefore, the corresponding linear peptide **20** was also not acetylated.

Sequential ligation

Cyclic and linear peptides were ligated onto the scaffold using a similar protocol as previously described⁸ with some improvements of the route. It appeared that the CuAAC reactions did not require microwave irradiation for completion. This also prevented the partial cleavage of the TES-group during the first ligation step. As a result the TES-deprotection step could be combined with the CuAAC step to ligate the first peptide on the scaffold (Scheme 3). After purification the TES-deprotected scaffolds (**22a-d**), with the first cyclic peptide attached, were obtained in good yields (45–67%).

Subsequently, the second cyclic peptide was ligated onto the scaffold with very good yields (**23a-d**, 63–84%). Removal of the TIPS-protecting group with TBAF, gave the free alkyne scaffolds (**24a-d**, 43–87%), to which the last cyclic peptide was ligated, which afforded the epitope mimics **25a-d** in 36–59% yields.

In total four epitope mimics were synthesized (Fig. 4). Three (**25a-c**) were based on cyclic peptides **16–18**. In these three mimics the order of introducing the peptides was varied as to evaluate the influence of the relative positions of the peptides. In addition, one more mimic (**20d**) was synthesized containing the linear peptides **19–21** to evaluate the relative influence of cyclic peptides and linear peptides on the biological activity of the mimics.

Biological activity

The three cyclic mimics (**25a-c**) were tested on their ability to competitively inhibit the interaction between CD4 and gp120 in an ELISA assay (Fig. 5). The procedure for this assay was described in our previous work.^{3a,b} This experiment showed little difference between the three mimics. All three showed good inhibition with IC₅₀ values between 41 and 57 μM (Table 1).



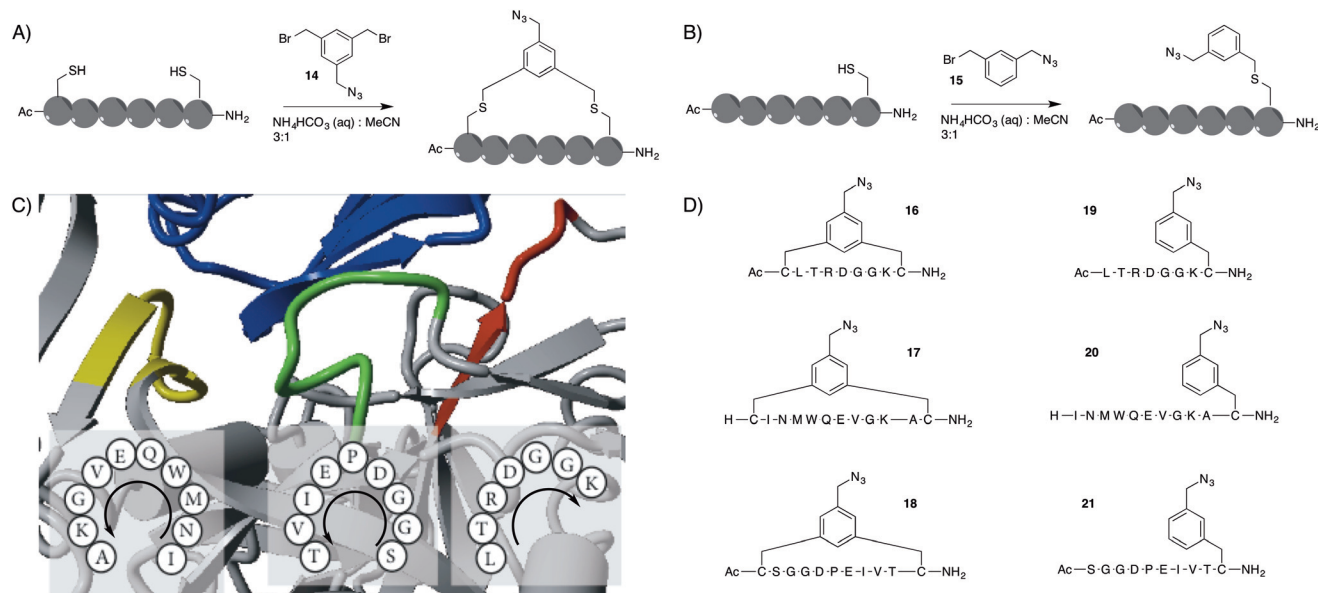
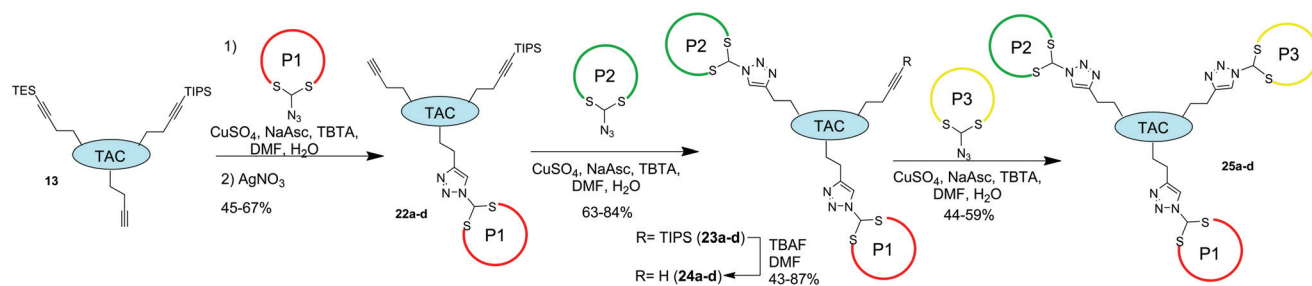


Fig. 3 (A) General scheme for the synthesis of azide-bearing cyclic peptide.⁸ (B) General scheme for the synthesis of azide-bearing linear peptides. (C) The three segments (yellow, green and red) of the HIV gp120 protein (gray) that are responsible for binding to CD4 (blue) are shown.⁷ Their amino acid residues and N → C direction are noted. (D) The cyclic (left) and linear (right) peptides that were synthesized according to (A) and (B) were based on the sequences of the HIV gp120 epitope (as shown in C).



Scheme 3 Sequential introduction of azide functionalized peptides onto the orthogonally protected tri-alkyne scaffold.

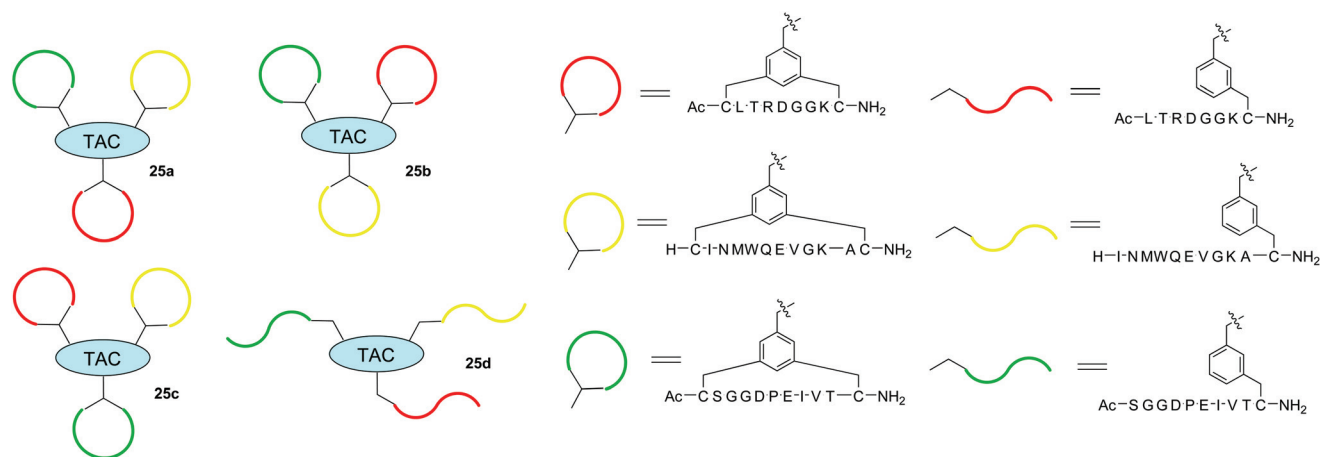


Fig. 4 Synthesized protein mimics 25a–d. Mimics 25a–c have the same three peptides attached, but the relative positioning of the peptides is different. Mimic 25d has the same relative positioning as mimic 25a but has linear peptides instead of cyclic.



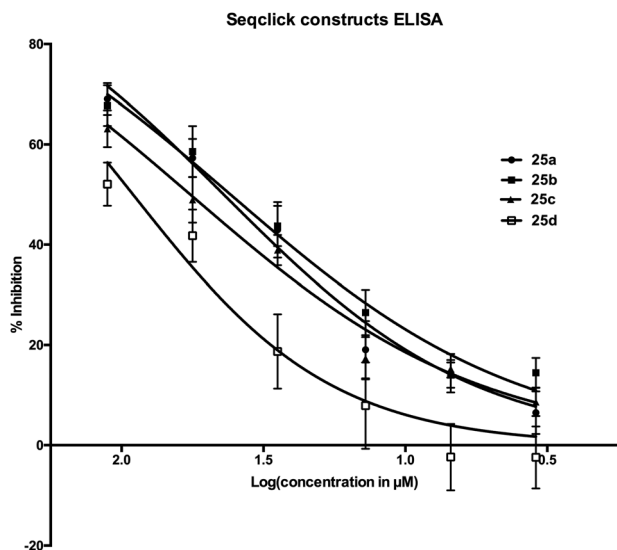


Fig. 5 Percentage of inhibition of binding of gp120 to CD4 by of the three discontinuous epitope mimics based on cyclic peptides (25a–c) and one based on linear peptides (25d) at different concentrations.

Table 1 IC₅₀ values for protein mimics 25a–d

	IC ₅₀ (μM)	Log IC ₅₀ with standard error
25a	43.7	1.64 ± 0.040
25b	41.3	1.62 ± 0.043
25c	57.3	1.76 ± 0.042
25d	91.1	1.96 ± 0.068

This suggests that the relative positioning of the peptides in the three gp120 protein mimics with respect to the CD4-receptor is similar. Possibly, the flexibility of the TAC-scaffold is at least partly responsible for a similar orientation of the three loops.

The epitope mimic based on linear peptides (25d) was also able to inhibit the binding of gp120 to CD4. However, the linear construct inhibits the binding to a lesser extent, with an about two-fold higher IC₅₀. This suggests that the use of cyclic of the peptides is beneficial for obtaining better protein mimics. This might be explained by an improved resemblance of cyclic peptides to the corresponding peptide segments, which are present in loop-like segments in the context of a protein. If more generally true this will improve mimicry possibilities of a protein binding site and therefore the development of reliable protein mimics.

To investigate the proteolytic stability of the constructs, compounds 25a and 25d were incubated with human serum (Fig. 6). Not entirely unexpected, compound 25a, consisting of scaffolded cyclic peptides, proved to be very stable and had hardly degraded after 24 hours, while compound 25d, consisting of scaffolded linear peptides, started to degrade already after 1 h and after 24 h only 25% remained intact. This result further underlines the importance of the use of cyclic

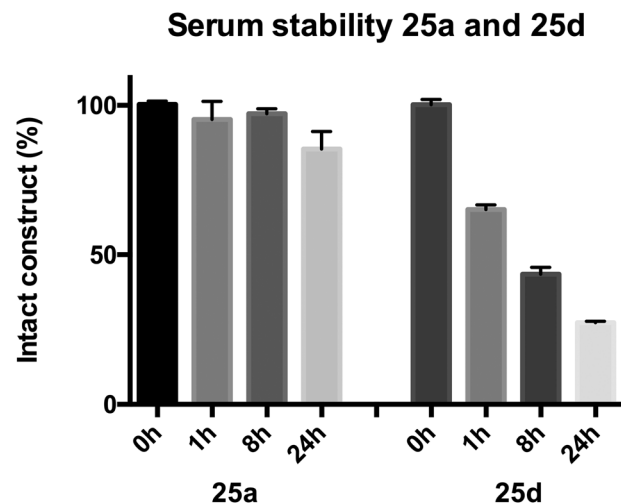


Fig. 6 Serum stability of constructs 25a and 25d.

peptides over linear peptides in order to obtain optimal protein mimics.

Conclusions

In this paper we have described an efficient and robust convergent route for the synthesis of protein mimics of discontinuous epitopes consisting of three loops on a suitable scaffold. The challenge here was the molecular construction of gp120 mimics encompassing the CD4 binding site. The resulting molecular constructs were adequate and capable of competing with gp120 for binding to the CD4 receptor. The relative position of the peptide loops had little influence on the ability to bind the CD4-receptor.

To investigate whether cyclic peptides have an advantage over linear we also synthesized a protein mimic based on linear peptides. This mimic was able to compete with gp120 for binding with CD4, but to a lesser extent than the cyclic peptide-based mimics. This shows the beneficial effect of the use of cyclic peptides on the bio-activity of the mimic and the importance of mimicking the conformation of the protein parts as closely as possible to obtain the best achievable protein mimic. The benefits of the use of cyclic peptides are underlined by the increased proteolytic stability of the constructs based on cyclic peptides as opposed to the constructs based on linear peptides.

We expect that this approach for the molecular construction of protein mimics is applicable to many other proteins in which several different peptide loops are crucial for their biological activity.

Experimental section

General information

Chemicals were obtained from commercial sources and used without further purification, unless stated otherwise. Peptide



grade DiPEA, CH₂Cl₂, NMP, TFA and HPLC grade solvents were purchased from Biosolve B.V. (Valkenswaard, The Netherlands). Fmoc-protected amino acids and BOP were purchased from GL Biochem Ltd (Shanghai, China). Used amino acids with side chain protecting groups were as follows: Fmoc-Arg(Pbf), Fmoc-Asp(OtBu), Fmoc-Cys(Trt), Fmoc-Gln(Trt), Fmoc-Glu(OtBu), Fmoc-His(Trt), Fmoc-Thr(tBu) and Fmoc-Trp(Boc). TentaGel S RAM resin (particle size 90 μm, capacity 0.25 mmol g⁻¹) was purchased from Rapp Polymere GmbH (Tübingen, Germany).

Solid phase peptide synthesis was performed on a C.S. Bio Co. peptide synthesizer (model CS336X). Unless stated otherwise, reactions were performed at room temperature. TLC analysis was performed on Merck precoated silica gel 60 F-254 plates. Spots were visualized with UV-light, ninhydrin stain (1.5 g ninhydrin and 3.0 mL acetic acid in 100 mL *n*-butanol), potassium permanganate (1.5 g of KMnO₄, 10 g K₂CO₃, and 1.25 mL 10% NaOH in 200 mL water) and/or molybdenum staining agent (12 g ammonium molybdate and 0.5 g ammonium cerium(IV) sulfate in 250 mL 10% H₂SO₄). Column chromatography was performed using Silica-P Flash silica gel (60 Å, particle size 40–63 μm) from Silicycle (Canada). Lyophilization was performed on a Christ Alpha 1–2 apparatus. ¹H NMR (400 MHz) and ¹³C NMR (100 MHz) experiments were conducted on a 300 MHz Varian G-300 spectrometer. Chemical shifts are given in ppm (δ) relative to TMS (0.00 ppm) (¹H NMR) or relative to CDCl₃ (77 ppm) (¹³C NMR).

Analytical HPLC was performed on a Shimadzu-10Avp (Class VP) system using a Phenomenex Gemini C18 column (110 Å, 5 μm, 250 × 4.60 mm) at a flow rate of 1 mL min⁻¹. The used buffers were 0.1% trifluoroacetic acid in MeCN/H₂O 5 : 95 (buffer A) and 0.1% trifluoroacetic acid in MeCN/H₂O 95 : 5 (buffer B). Runs were performed by a standard protocol: 100% buffer A for 2 min, then a linear gradient of buffer B (0–100% in 48 min) and UV-absorption was measured at 214 and 254 nm. Purification by preparative HPLC was performed on a Prep LCMS QP8000α HPLC system (Shimadzu) using a Phenomenex Gemini C18 column (10 μm, 110 Å, 250 × 21.2 mm) at a flow rate of 12.5 mL min⁻¹. Runs were performed by a standard protocol: 100% buffer A for 5 min followed by a linear gradient of buffer B (0–100% in 70 min) with the same buffers as were described for analytical HPLC.

ESI-TOF MS spectra were recorded on a microTOF mass spectrometer (Bruker). Samples were diluted with tuning mix (1 : 1, v/v) and infused at a speed of 300 μL h⁻¹ using a nebulizer pressure of 5.8 psi, a dry gas flow of 3.0 L min⁻¹, a drying temperature of 180 °C and a capillary voltage of 5.5 kV. Analytical LC-MS (electrospray ionization) was performed on ThermoFinnigan LCQ Deca XP Max using same buffers and protocol as described for analytical HPLC. All reported mass values are monoisotopic.

The microtiterplate reader used in the ELISA assays was a BioTek μQuant (Beun de Ronde, Abcoude, The Netherlands).

Scaffold synthesis

***tert*-Butyl pent-4-ynoate (2).**¹³ According to literature procedure, 1,4-pentynoic acid (1, 5.0 g, 51.0 mmol), *t*-BuOH

(9.7 mL, 101.8 mmol) and DMAP (0.3 g, 2.5 mmol) were dissolved in CH₂Cl₂ (10 mL). The mixture was stirred for 10 min. A solution of DCC (11.55 g, 56.0 mmol) in CH₂Cl₂ (10 mL) was added and the resulting mixture was stirred overnight. Next the formed precipitate was removed by filtration and washed with CH₂Cl₂. The filtrate was washed with 0.5 M HCl (2 × 100 mL), 1 M NaHCO₃ (2 × 100 mL) and dried over Na₂SO₄. The mixture was filtered and the solvent was removed by evaporation. The residue was purified by silica gel column chromatography (CH₂Cl₂) to give *tert*-butyl pent-4-ynoate (2) as a yellowish oil (6.3 g, 40.8 mmol, 80%). Spectroscopic data was in agreement with literature data.¹³

***tert*-Butyl 5-(triisopropylsilyl)pent-4-ynoate (3a).** Compound 2 (1.0 g, 6.5 mmol) was dissolved in anhydrous THF (20 mL) and cooled to –78 °C with a dry ice and acetone bath. *n*-BuLi (2.6 mL, 2.5 M in hexane, 6.5 mmol) was added dropwise and the reaction mixture was stirred for 10 minutes. Then the dry ice/acetone bath was replaced with an ice bath (0 °C) and TIPS-Cl (1.7 mL, 7.8 mmol) was added dropwise. The reaction mixture was stirred for 3 hours at room temperature, after which it was quenched with 40 mL saturated aqueous NH₄Cl. THF was removed by evaporation *in vacuo* and the resulting aqueous slurry was diluted with H₂O (50 mL). The mixture was extracted with EtOAc (3 × 30 mL) and the combined organic layers were dried over Na₂SO₄. After filtration, the solvent was evaporated. The crude product was purified by silica gel column chromatography (eluent: 10% Et₂O in hexanes) to give *tert*-butyl 5-(triethylsilyl)pent-4-ynoate (3a) as a yellow oil (1.4 g, 4.4 mmol, 68%). *R*_f = 0.55 (5% EtOAc in petroleum ether 40–60). ¹H NMR (400 MHz, CDCl₃): δ = 1.04 (m, 21H, CH(CH₃)₂), 1.44 (s, 9H, C(CH₃)₃), 2.44–2.54 (m, 4H, CH₂CH₂). ¹³C NMR (100 MHz, CDCl₃): δ = 11.2 (CH(CH₃)₂), 15.9 (C(O)CH₂CH₂), 18.6 (CH(CH₃)₂), 28.1 (C(CH₃)₃), 35.1 (C(O)CH₂), 80.6, 80.8 (CCH₃, CCSi), 107.1 (CCSi), 171.1 (C=O).

***tert*-butyl 5-(triethylsilyl)pent-4-ynoate (3b).** Compound 2 (1.4 g, 9.3 mmol) was dissolved in anhydrous THF (20 mL) and cooled to –78 °C with a dry ice and acetone bath. *n*-BuLi (3.7 mL, 2.5 M in hexane, 9.3 mmol) was added dropwise and the reaction mixture was stirred for 10 minutes. Then the dry ice/acetone bath was replaced with an ice bath (0 °C) and TES-Cl (1.9 mL, 11.2 mmol) was added dropwise. The reaction mixture was stirred for 3 hours at room temperature, after which it was quenched with 40 mL aqueous saturated NH₄Cl. THF was removed by evaporation *in vacuo* and the resulting aqueous slurry was diluted with H₂O (50 mL). The mixture was extracted with EtOAc (3 × 30 mL) and the combined organic layers were dried over Na₂SO₄. After filtration, the solvent was evaporated. The crude product was purified by silica gel column chromatography (eluent: 2% EtOAc in hexanes) to give *tert*-butyl 5-(triethylsilyl)pent-4-ynoate (3b) as a yellow oil (1.8 g, 6.7 mmol, 72%). *R*_f = 0.54 (5% EtOAc in petroleum ether 40–60). ¹H NMR (400 MHz, CDCl₃): δ = 0.55 (*q*, *J* = 8 Hz, 6H, CH₂–CH₃), 0.96 (*t*, *J* = 8 Hz, 9H, CH₂–CH₃), 1.45 (*s*, 9H, CCH₃), 2.43–2.53 (*m*, 4H, CH₂–CH₂). ¹³C NMR (100 MHz, CDCl₃): δ = 4.4 (CH₂–CH₃), 7.4 (CH₂–CH₃), 15.9 (C(O)CH₂–CH₂), 28.0



(CCH₃), 35.0 (C(O)CH₂) 80.6, 82.2 (CCH₃, CCSi), 106.5 (CCSi), 171.1 (C=O).

5-(Triisopropylsilyl)4-pentynoic acid (4a). Compound **3a** (1.3 g, 4.3 mmol) was dissolved in 15% TFA in CH₂Cl₂ (50 mL) and the resulting mixture was stirred for 2 hours. The mixture was then quenched with 1 M ammonium acetate (100 mL) and extracted with CH₂Cl₂ (2 × 75 mL). The combined organic layers were dried over Na₂SO₄, filtered and evaporated. The crude product was purified by silica gel column chromatography (10% Et₂O in hexanes). 5-(Triethylsilyl)4-pentynoic acid (**4a**) was obtained as a yellow oil (1.1 g, 4.1 mmol, 97%). *R*_f = 0.33 (30% EtOAc in hexanes). ¹H NMR (400 MHz, CDCl₃): δ 1.05 (m, 21H, CH(CH₃)₂), 2.56–2.64 (m, 4H, CH₂–CH₂). ¹³C NMR (100 MHz, CDCl₃): δ 11.2 (CH₂–CH₃), 15.6 (C(O)CH₂–CH₂), 18.5 (CH₂–CH₃), 33.7 (C(O)CH₂), 81.6 (CCSi), 106.2 (CCSi), 177.3 (C=O).

5-(Triethylsilyl)4-pentynoic acid (4b). Compound **3b** (1.8 g, 6.7 mmol) was dissolved in 15% TFA in CH₂Cl₂ (50 mL) and the resulting mixture was stirred for 2 hours. The mixture was then quenched with 1 M ammonium acetate (100 mL) and extracted with CH₂Cl₂ (2 × 75 mL). The combined organic layers were dried over Na₂SO₄, filtered and evaporated. The crude product was purified by silica gel column chromatography (eluent: 10% Et₂O in hexanes). 5-(Triethylsilyl)4-pentynoic acid (**4b**) was obtained as a yellow oil (0.55 g, 2.6 mmol, 39%). *R*_f = 0.34 (10% EtOAc in hexanes). ¹H NMR (400 MHz, CDCl₃): δ = 0.56 (q, *J* = 8 Hz, 6H, CH₂–CH₃), 0.97 (t, *J* = 8 Hz, 9H, CH₂–CH₃), 2.53–2.63 (m, 4H, CH₂–CH₂). ¹³C NMR (100 MHz, CDCl₃): δ = 4.4 (CH₂–CH₃), 7.4 (CH₂–CH₃), 15.6 (C(O)CH₂–CH₂), 33.5 (C(O)CH₂), 82.9 (CCSi), 105.6 (CCSi), 171.1 (C=O).

N-(3-Bromopropyl)-2-nitrobenzene-sulfonamide (6).¹⁴ According to literature procedure,¹⁴ 3-bromo-propylamine hydrobromide (5, 15.0 g, 68.5 mmol) and 2-nitrobenzene-sulfonyl chloride (18.2 g, 82.2 mmol) were dissolved in CH₂Cl₂ (180 mL) and cooled to 0 °C. After adding TEA (21.9 mL, 164.4 mmol) the mixture was stirred at room temperature for 3 hours. The mixture was washed with 1 M HCl (50 mL), brine (50 mL) and H₂O (50 mL). The organic phase was dried over Na₂SO₄, filtered and the solvent was removed under vacuum to yield the product as a white solid (21.57 g, 66.7 mmol, 97%). Spectroscopic data was in agreement with literature data.¹⁴

oNBS and TFA protected triamine with pentynoic acid residue 9. For the synthesis of crude compound **8** a literature procedure was followed.¹⁰

To a cooled solution of 1,3 diaminopropane (25.8 mL 309 mmol) in DMA (200 mL) a solution of sulfonamide bromide **6** (10.0 g, 30.9 mmol) in DMA (50 mL) was added dropwise. The resulting mixture was stirred overnight at room temperature. An aqueous solution of 4 M NaOH (aq, 7.7 mL, 30.9 mmol) was added and the mixture was concentrated *in vacuo* to ca. a third of the volume. DMA (100 mL) was added and again the mixture was concentrated until a third of the volume remained. This co-evaporation was repeated until the collected DMA was not basic anymore due to remaining diaminopropane (pH indicator paper). After

evaporation of the remaining DMA triamine **7** was obtained as a yellow oil.

To crude intermediate **7** MeCN (150 mL), H₂O (0.7 mL, 38.8 mmol) and CF₃CO₂Et (18.5 mL, 155.2 mmol) were added. After overnight stirring under reflux the mixture was concentrated *in vacuo* to afford the crude TFA-protected triamine (**8**) as a yellow oil.

Crude compound **8** was dissolved in CH₂Cl₂ (200 mL). BOP (14.3 g, 32.3 mmol), 4-pentynoic acid (3.0 g, 30.8 mmol) and NMM (10.4 mL, 95.5 mmol) were added and the mixture was stirred overnight. The solvent was evaporated and the residue was dissolved in EtOAc (100 mL) and washed with 5% NaHCO₃ (2 × 100 mL), 1 M of KHSO₄ (2 × 100 mL) and brine (100 mL). The organic layer was dried over Na₂SO₄ and filtered and the solvent was removed by evaporation. Silica gel column chromatography (eluent: EtOAc/hexane; 1/1 until removal of the first yellow band, then 6/4 until the product started to elute and 7/3 to complete the elution of the product) afforded triamine **9** as a yellow/orange oil (9.53 g, 19.4 mmol, 63%). *R*_f = 0.61 (20% hexanes in EtOAc). ¹H NMR (400 MHz, CDCl₃): δ 1.67–1.76, 1.83–1.92 (2m, 4H, N–CH₂–CH₂), 1.96 (s, 1H, CCH), 2.54 (m, 4H, C(O)–CH₂–CH₂), 3.05–3.18, 3.22–3.34 (2m, 4H, 2 × NH–CH₂–CH₂), 3.38–3.45 (m, 4H, CH₂–N–CH₂), 5.51, 6.19, 6.74 (3m, 2H, NH), 7.69–7.90, 8.07–8.15 (2m, 4H, Ar–H). ¹³C NMR (100 MHz, CDCl₃): δ = 14.7, 14.9, 31.7, 31.9 (N–C(O)–CH₂–CH₂), 26.8, 28.1, 28.5, 29.0 (2 × CH₂–CH₂–CH₂), 35.8, 40.8, 41.0, 45.4 (2 × NH–CH₂–CH₂), 37.4, 42.2, 42.8, 45.0 (2 × CH₂–N–CH₂), 68.9, 69.2, 82.9, 83.1(C–CH), 114.5, 117.4 (CF₃), 125.1, 125.5, 130.7, 131.0, 132.6, 132.9, 133.2, 133.4, 133.9 (Ar–C), 148.1 (CNO₂), 157.1, 157.5 (CF₃–C=O), 171.6, 172.5 ((CH₂)₂NC=O). Exact mass calculated [M + H]⁺: *m/z* 493.1369 g mol⁻¹. Mass measured: *m/z* 493.1344 g mol⁻¹.

Triamine cyclization (11). Dibromide **10** was obtained according to a literature procedure.¹¹

Triamine **9** (3.0 g, 6.1 mmol), dibromide **10** (2.0 g, 6.1 mmol) and Cs₂CO₃ (8.0 g, 24.4 mmol) were dissolved in DMF (500 mL) and the resulting mixture was stirred overnight. After evaporation of DMF both EtOAc (300 mL) and H₂O (180 mL) were added. The organic layer was washed with an aqueous solution of 1 M KHSO₄ (200 mL) and with brine (200 mL), dried over Na₂SO₄ and filtered. Concentration *in vacuo* afforded the crude product as an orange oil which was purified using silica gel column chromatography (eluent: 2% acetone in CH₂Cl₂). Compound **11** was obtained as a yellow to orange foam (2.7 g, 4.1 mmol, 67%). *R*_f = 0.38 (EtOAc/Hexanes, 7 : 3). ¹H NMR (400 MHz, CDCl₃): δ 1.23–1.45, 1.60–1.70 (2m, 4H, 2 × N–CH₂–CH₂), 1.92 (m, 1H, CCH), 2.435–2.47 (m, 4H, C(O)–CH₂–CH₂), 3.93, 3.95 (2s, 3H, OCH₃), 4.38–4.53, 4.63–4.80 (2m, 4H, 2 × Ar–CH₂–N), 7.65–8.11 (m, 7H, ArH). Exact mass calculated [M + H]⁺: *m/z* 653.1893 g mol⁻¹. Mass measured: *m/z* 653.1879 g mol⁻¹.

Pentynoic acid amidated TAC-scaffold 12. Compound **11** (1.7 g, 2.6 mmol) was dissolved in dioxane/MeOH/aq NaOH (4 M) (15 : 4 : 1, 91 mL, 18.2 mmol) and the resulting mixture was stirred overnight. 1 M HCl was added until the mixture was pH neutral (pH indicator paper), after which MeCN



(50 mL) and H₂O (50 mL) were added. The pH was adjusted to approximately 8 using DiPEA (using a pH electrode) and a solution of Fmoc-OSu (0.95 g, 2.8 mmol) in MeCN. This was followed by the dropwise addition of DiPEA to maintain the pH at 8. The reaction was considered complete when no more DiPEA was needed to keep the pH above 7.5 for 10 min. Addition of aqueous solution of HCl (1 M, 30 mL) and H₂O (200 mL) was followed by extraction with EtOAc (2 × 200 mL). The combined organic layers were washed with brine and dried over Na₂SO₄. Evaporation of the solvents gave the crude compound which was purified using silica gel column chromatography (gradient from EtOAc/Hexanes/AcOH 8/2/0.1 to 0.1% AcOH in EtOAc to give the Fmoc-protected TAC-scaffold (**12**) (1.6 g, 2.1 mmol, 80%) $R_f = 0.37$ (6% MeOH/CH₂Cl₂). Exact mass calculated [M + H]⁺: m/z 765.2594 g mol⁻¹. Mass measured: m/z 765.2618 g mol⁻¹.

Orthogonally protected trialkyne TAC-scaffold 13. TAC-scaffold **12** (0.3 g, 0.4 mmol) was dissolved in CH₂Cl₂ (20 mL) and DiPEA (70 μL, 0.4 mmol) and 2-chlorotriptyl chloride resin (1.0 g, 3.2 mmol) were added. After 5 minutes DiPEA (105 μL, 0.6 mmol) was added and the mixture was stirred overnight. DiPEA (1 mL) and MeOH (4 mL) were added and the mixture was stirred for 30 minutes. The resin was transferred to a solid phase synthesis tube and washed with MeOH (3 × 20 mL) and Et₂O (3 × 20 mL). After drying for 30 minutes, 5 mg of resin was transferred to a 20 mL volumetric flask and 20% piperidine in NMP (2 mL) was added. The flask was shaken for 30 minutes after which MeOH was added until a volume of 20 mL. UV-absorption was measured at 300 nm resulting in a loading of 0.25 mmol g⁻¹ resin (loading yield of 63%). The resin was washed with CH₂Cl₂ (3 × 20 mL), NMP (3 × 20 mL) and 20% piperidine/NMP (20 mL) was added. The mixture was bubbled through with N₂ for 30 minutes, followed by washing with NMP (3 × 20 mL) and CH₂Cl₂ (3 × 20 mL). A positive Bromophenol Blue-test indicated Fmoc removal.

Next, BOP (0.22 g, 0.5 mmol), CH₂Cl₂ (20 mL), TIPS-protected pentynoic acid **4a** (0.13 g, 0.5 mmol), DiPEA (1.7 mL, 1.0 mmol) were added respectively. The mixture was bubbled through with N₂ for 2 hours. Then the resin was washed with CH₂Cl₂ (3 × 20 mL). A negative Bromophenol Blue-test indicated coupling of the pentynoic acid derivative.

The resin was washed with DMF (3 × 20 mL). DMF (20 mL), β-mercaptoethanol (175 μL, 2.5 mmol) and DBU (187 μL, 152.24 g mol⁻¹, 1.25 mmol, 1.02 g cm⁻³, 5 equiv.) were added subsequently. The mixture was bubbled through with N₂ for 15 minutes. The deprotection step was repeated once. The resin was washed with DMF (3 × 20 mL) and CH₂Cl₂ (3 × 20 mL). A positive Bromophenol Blue-test indicated oNBS removal.

Next, BOP (0.22 g, 0.5 mmol), CH₂Cl₂ (20 mL), TES-protected pentynoic acid **4b** (0.11 g, 0.5 mmol) and DiPEA (166.8 μL, 1.0 mmol) were added and the mixture was bubbled through with N₂ for 2 hours. The resin was washed with CH₂Cl₂ (3 × 20 mL) and a negative Bromophenol Blue-test indicated coupling of the pentynoic acid derivative. The resin was transferred to a round-bottom flask and 30% HFIP in CH₂Cl₂

(20 mL) was added. The mixture was allowed to stir for 45 minutes. After filtration and washing of the residue with CH₂Cl₂, EtOAc (30 mL) was added to the filtrate. The solvents were removed by evaporation. Silica gel column chromatography (6% MeOH in CH₂Cl₂) afforded scaffold **13** as a colorless oil. The oil was dissolved in *t*-BuOH/H₂O and lyophilized to obtain a white solid (0.15 g, 0.19 mmol, 76%). $R_f = 0.55$ (10% MeOH in CH₂Cl₂). ¹H NMR (400 MHz, CDCl₃): δ = 0.57 (q, $J = 7.9$ Hz, 6H, 3 × CH₂CH₃), 0.97 (t, $J = 7.9$ Hz, 9H, 3 × CH₂CH₃), 1.04 (m, 21H, 3 × CH(CH₃)₂), 1.32–1.60 (m, 4H, N-CH₂-CH₂-CH₂-N), 1.92 (m, 1H, CCH), 2.44 (m, 4H, CH₂CH₂CCH), 2.60–2.78 (m, 8H, 2 × CH₂CH₂CCSi), 2.81–3.08, 3.40–3.50 (2m, 8H, N-CH₂-CH₂-CH₂-N), 4.59–4.72 (m, 4H, 2 × N-CH₂-Ar). ¹³C NMR (100 MHz, CDCl₃): δ = 4.4 (SiCH₂), 7.5 (SiCH₂CH₃), 11.2 (SiCH), 14.5, 14.5 (CH₂CCH), 16.3, 16.4 (CH₂CCSi), 18.6 (SiCH(CH₃)₂), 28.0, 28.0, 28.3 (CH₂CH₂CH₂), 31.9, 31.9 (CH₂CH₂CCH), 32.8, 33.1, 33.1 (CH₂CH₂CCSi), 43.5, 45.5, 45.6, 45.7, 46.0, 48.2, 48.3 (NCH₂CH₂CH₂N), 52.0, 52.1, 53.8, 53.8 (ArCH₂N), 68.8 (CCH), 81.2, 81.3, 82.7, 82.7, 83.1, 83.2 (CCH, CCSi), 106.4, 106.4, 107.0, 107.0 (CCSi), 128.8, 130.0, 130.0, 130.1, 130.3, 131.1, 131.2, 131.5, 131.6, 138.2, 140.5 (ArC), 168.9, 170.7, 172.0, 172.5 (C=O). Exact mass calculated [M + H]⁺: m/z 788.4854 g mol⁻¹. Mass measured: m/z 788.4831 g mol⁻¹.

1-(Azidomethyl)-3-(bromomethyl)-benzene (15). 1,3-Bis(bromomethyl)-benzene (1.32 g, 5.00 mmol) was dissolved in DMF (40 mL), followed by the dropwise addition of a suspension of NaN₃ (0.29 g, 4.46 mmol, 0.9 eq.) in DMF (10 mL). The resulting mixture was stirred for 3 h and the reaction was monitored using TLC (10% EtOAc in hexanes). Upon completion of the reaction, the mixture was concentrated *in vacuo*, which yielded a yellow oil that contained NaBr-salt precipitation. The oil was dissolved in EtOAc and the resulting mixture was filtered. The filtrate was concentrated *in vacuo* and purified using silica gel column chromatography (0.5% EtOAc in hexanes), which yielded the product as a clear light yellow oil. Despite multiple purification attempts, 1,3-bis(azidomethyl)-benzene remained as an impurity. Analysis by ¹H-NMR provided a ratio of 70:30 for 1-(azidomethyl)-3-(bromomethyl)-benzene (**15**) and 1,3-bis(azidomethyl)-benzene, respectively. Yield: 0.72 g (of which 0.53 g monoazide). R_f (monoazide: 0.63 (10% EtOAc in PE). ¹H-NMR (400 MHz, CDCl₃): δ = 4.35, 4.36 (s, 2H, CH₂N) 4.49 (s, 2H, CH₂Br), 7.23–7.40 (m, 4H, Ar-H). ¹³C-NMR (100 MHz, CDCl₃): δ = 32.97 (CH₂Br), 54.43, 54.50 (CH₂N₃), 127.80, 128.01, 128.10, 128.66, 128.90, 129.31, 129.34, 136.13, 136.15, 138.47 (Ar-C).

Peptide synthesis

Solid phase peptide synthesis. Linear peptides were synthesized on a C.S. Bio Co. peptide synthesizer using Tentagel S RAM resin (linker amide linker) on a 0.25 mmol scale. Fmoc-deprotection was performed using 20% piperidine in NMP. Fmoc-deprotection was monitored by piperidine–benzofulvene adduct fluorescence using an UV-detector (305 nm). If a significant amount of the piperidine–benzofulvene adduct was detected in the second deprotection step a double coupling of



the subsequent amino acid was performed. Amino acids are coupled using 4 equiv. of amino acid and HBTU as activating agent with DiPEA as base and NMP as solvent. Capping was performed using acetic anhydride (12 mL), HOBT (50 mg) and DiPEA (5.5 mL) in NMP (250 mL). Note: for peptides containing a Asp-Gly sequence (*i.e.* **16** and **19**) that glycine residue was coupled as Fmoc-(Dmb)-Gly-OH to prevent aspartimide formation.

General procedure for the cleavage and deprotection of the linear peptide from the solid support. The sidechain-protected linear peptide was cleaved from the resin and deprotected using a mixture of TFA : H₂O : EDT : TIS (90 : 5 : 2.5 : 2.5) (v/v/v/v), 10 mL per gram resin. The reaction mixture was stirred for 3 hours after which the mixture was concentrated to a volume of 2 mL, followed by precipitation of the peptides from MTBE/hexane (1 : 1 v/v). After centrifugation (3500 rpm, 5 min), the supernatant was decanted and the pellet was re-suspended in MTBE/hexane (1 : 1 v/v) and centrifuged again. The pellet was dissolved in *t*-BuOH/H₂O (1 : 1 v/v) and lyophilized. The purity of the peptides was analyzed by analytical HPLC and the peptides were characterized with by spectrometry.

Alkylation of cysteine residues.⁸ Crude peptide was dissolved in 20 mM NH₄HCO₃ (aq)/MeCN (3/1 (v/v)) (80 mL). Crude 1-azido-3-bromo-xylylene (**14**) or 1-(azidomethyl)-3,5-bis-(bromomethyl)-benzene (**15**) was dissolved in MeCN (5 mL) and the resulting solution was added dropwise to the crude peptide solution. The resulting mixture was stirred for 3 h and the reaction was monitored using LC/MS. Upon completion of the reaction, the mixture was concentrated *in vacuo*. The mixture was lyophilized overnight, which yielded the crude product as a fluffy white powder. The crude product was purified using preparative HPLC.

Sequential ligation

General procedure for first cycloaddition and subsequent TES-removal 22a–d. Solutions of TAC-scaffold **13** (7.9 mg, 10 μmol) in 100 μL DMF, the peptide loop (10 μmol) in 100 μL DMF, CuSO₄·5H₂O (3 μmol, 0.75 mg) in 100 μL H₂O, NaAsc (9 μmol, 1.8 mg) in 100 μL H₂O and TBTA (1.5 μmol, 0.8 mg) in 100 μL DMF were prepared (if needed the solutions of CuSO₄, NaAsc and TBTA were prepared as 10-fold solution in 1 mL). The five solutions were combined and DMF (0.9 mL) and H₂O (0.6 mL) were added to obtain a final volume of 2 mL of DMF/H₂O 3/2 (v/v). The resulting mixture was stirred at room temperature for 3 hours and the progress of the reaction was monitored using LC-MS. When the reaction was complete a solution of AgNO₃ (100 μmol, 17.0 mg) in H₂O (0.5 mL) was added and the mixture was stirred at room temperature for 1 hour. The mixture was then diluted to a volume of 5 mL with MeCN/H₂O/TFA (50/50/0.1), followed by the addition of NaCl (100 μmol, 5.8 mg) in order to remove Ag⁺ as an AgCl precipitate. The formed suspension was centrifuged (5 min, 5000 rpm) and the supernatant was purified using preparative HPLC. The product-containing fractions were pooled and lyophilized to obtain the TES-deprotected scaffold as a white solid.

General procedure for the conjugation of the second peptide onto the scaffold (23a–d). Solutions of the scaffold – containing one peptide sequence and one free and one protected alkyne – (5 μmol 1 equiv.) in 200 μL DMF and of the peptide (5 μmol, 1 equiv.) in 200 μL DMF were prepared. Stock solutions of CuSO₄·5H₂O (15 μmol, 3 equiv. in 1 mL H₂O), NaAsc (45 μmol, 9 equiv. in 1 mL H₂O) and TBTA (15 μmol, 1.5 equiv. in 1 mL DMF) were prepared. The solutions of the scaffold and the peptide were combined and 100 μL each of the CuSO₄, the NaAsc and TBTA solutions was added. To the resulting mixture DMF (0.4 mL) and H₂O (0.4 mL) were added to obtain a final volume of 1.5 mL of DMF/H₂O 3 : 2 (v/v). The resulting mixture was stirred at room temperature (usually for 3 h) and the progress of the reaction was monitored by LC-MS. When the reaction was complete, the mixture was diluted to a volume of 5 mL with MeCN/H₂O/TFA (50/50/0.1). The resulting mixture was centrifuged (5 min, 5000 rpm) and the supernatant was purified using preparative HPLC. The product-containing fractions were pooled and lyophilized to obtain the TAC-scaffold with as a white solid.

General procedure for the removal of the TIPS-protecting group (24a–d). The TIPS-protected scaffold (5 μmol) was dissolved in DMF (1 mL) and a solution of TBAF·3H₂O (50 μmol, 10 equiv.) was added. The resulting mixture was stirred at room temperature and the progress was monitored by LC-MS. When the reaction was complete (usually after stirring overnight), the mixture was diluted to a volume of 5 mL with MeCN/H₂O/TFA (50/50/0.1). The resulting mixture was centrifuged (5 min, 5000 rpm) and the supernatant was purified using preparative HPLC. The product-containing fractions were pooled and lyophilized to obtain the product as a white solid.

General procedure for the conjugation of the third peptide onto the scaffold (25a–e). Solutions of the scaffold – containing two peptides and one free alkyne – (5 μmol 1 equiv.) in 200 μL DMF and of the peptide (5 μmol, 1 equiv.) in 200 μL DMF were prepared. Stock solutions of CuSO₄·5H₂O (15 μmol, 3 equiv. in 1 mL H₂O), NaAsc (45 μmol, 9 equiv. in 1 mL H₂O) and TBTA (7.5 μmol, 1.5 equiv. in 1 mL DMF) were prepared. The solutions of the scaffold and the peptide were combined and 100 μL each of the CuSO₄, the NaAsc and TBTA solutions was added. To the resulting mixture DMF (0.4 mL) and H₂O (0.4 mL) were added to obtain a final volume of 1.5 mL of DMF/H₂O 3 : 2 (v/v). The resulting mixture was stirred at room temperature (usually for 3 h) and the progress of the reaction was monitored by LC-MS. When the reaction was complete, the mixture was diluted to a volume of 5 mL with MeCN/H₂O/TFA (50/50/0.1). The resulting mixture was centrifuged (5 min, 5000 rpm) and the supernatant was purified using preparative HPLC. The product-containing fractions were pooled and lyophilized to obtain the product as a white solid.

HIV-1 gp120 capture ELISA

Recombinant HIV-1IIIB gp120 protein (referred to as rgp120 hereafter unless otherwise noted) capture ELISA was performed according to the manufacturer's instructions (ImmunoDiagnostics, Inc., Woburn, MA). A solution of the test



compound, diluted in sample buffer (50 μL 0.1% BSA in PBS) and 2% DMSO, was added to the CD4-coated plate, which was immediately followed by the addition of 50 μL 2 $\mu\text{g mL}^{-1}$ rgp120 (final concentration 1 $\mu\text{g mL}^{-1}$). After 4 hours incubation at room temperature, the plate was washed with wash buffer (0.1% Tween 20 in PBS) followed by incubation with peroxidase-conjugated murine anti-gp120 MAb to detect the amounts of captured rgp120. Any unbound material was washed away using wash buffer, and the plates were developed by adding 100 μL per well substrate solution (0.1 mg mL^{-1} TMB in 0.1 N NaOAc buffer pH 5.5, containing 0.003% H_2O_2). The reaction was stopped by adding 100 μL 4 N sulfuric acid. Absorbances (ODs) were read at 450 nm using a microtiterplate reader. All assays were performed in duplicate and all compounds were tested independently at least three times.

Serum stability assay

4 mg mL^{-1} construct solutions were prepared in MilliQ. Duplicate samples were prepared with 100 μL peptide solution and 500 μL human serum. The samples were incubated at 37 $^\circ\text{C}$, and samples were taken at $t = 0, 1, 8$ and 24 h as follows: to 100 μL serum solution, 200 μL MeOH (containing 0.075 mg mL^{-1} ethylparaben as an internal standard) was added to precipitate the proteins. The sample was vortexed briefly and allowed to stand for 10 min at RT. The samples were then centrifuged at 12 000 rpm for 5 min, and the supernatant was taken and stored at -20 $^\circ\text{C}$ until analysis. Each sample was analyzed by HPLC, on a C18 column. The peaks were integrated and normalized to the internal standard.

Acknowledgements

This research was financed by Chemical Sciences of the Netherlands Organization for Scientific Research (NWO). We gratefully acknowledge Javier Sastre Torano for the MS measurements.

Notes and references

- (a) T. Opatz and R. M. J. Liskamp, *Org. Lett.*, 2001, **3**, 3499; (b) E. T. Rump, D. T. S. Rijkers, H. W. Hilbers, P. G. de Groot and R. M. J. Liskamp, *Chem. – Eur. J.*, 2002, **8**, 4613.
- (a) C. Chamorro and R. M. J. Liskamp, *J. Comb. Chem.*, 2003, **5**, 794; (b) M. Hijnen, D. J. van Zoelen, C. Chamorro, P. Gageldonk, F. R. Mooi, G. Berbers and R. M. J. Liskamp, *Vaccine*, 2007, **25**, 6807; (c) C. Chamorro, J. A. W. Kruijtzter, M. Farsaraki, J. Balzarini and R. M. J. Liskamp, *Chem. Commun.*, 2009, 821; (d) H. van de Langemheen, H. C. Quarles van Ufford, J. A. W. Kruijtzter and R. M. J. Liskamp, *Org. Lett.*, 2014, **16**, 2138.
- (a) G. E. Mulder, J. A. W. Kruijtzter and R. M. J. Liskamp, *Chem. Commun.*, 2012, **48**, 10007; (b) G. E. Mulder, H. C. Quarles van Ufford, J. van Ameijde, A. J. Brouwer, J. A. W. Kruijtzter and R. M. J. Liskamp, *Org. Biomol. Chem.*, 2013, **11**, 2676; (c) H. van de Langemheen, M. van Hoeke, H. C. Quarles van Ufford, J. A. W. Kruijtzter and R. M. J. Liskamp, *Org. Biomol. Chem.*, 2014, **12**, 4471.
- D. J. Craik, D. P. Fairlie, S. Liras and D. Price, *Chem. Biol. Drug Des.*, 2013, **81**, 136.
- C. Chamorro and R. M. J. Liskamp, *J. Comb. Chem.*, 2003, **5**, 794.
- (a) R. Franke, T. Hirsch and J. Eichler, *J. Recept. Signal Transduction*, 2006, **26**, 453; (b) A. Groß, K. Rödel, B. Kneidl, N. Dornhauser, M. Mössl, E. Lump, J. München, B. Schmidt and J. Eichler, *ChemBioChem*, 2015, **16**, 446; (c) Y. Singh, G. Dolphin, J. Razkin and P. Dumy, *ChemBioChem*, 2006, **7**, 1298; (d) O. Avrutina, M. Empting, S. Fabritz, M. Daneschdar, H. Frauendorf, U. Diedrichsen and H. Kolmar, *Org. Biomol. Chem.*, 2009, **7**, 4177.
- P. D. Kwong, R. Wyatt, S. Majeed, J. Robinson, R. W. Sweet, J. Sodroski and W. A. Hendrickson, *Structure*, 2000, **8**, 1329.
- P. R. Werkhoven, H. van de Langemheen, S. van der Wal, J. A. W. Kruijtzter and R. M. J. Liskamp, *J. Pept. Sci.*, 2014, **20**, 235.
- I. E. Valverde, A. F. Delmas and V. Aucagne, *Tetrahedron*, 2009, **65**, 7597.
- A. J. Brouwer, H. van de Langemheen and R. M. J. Liskamp, *Tetrahedron*, 2014, **70**, 4002.
- K. Kurz and M. W. Göbel, *Helv. Chim. Acta*, 1996, **79**, 1967.
- P. Timmerman, J. Beld, W. C. Puijk and R. H. Meloen, *ChemBioChem*, 2005, **6**, 821.
- G. M. Fischer, C. Jüngst, M. Isomäki-Krondahl, D. Gauss, H. M. Möller, E. Daltrozzo and A. Zumbusch, *Chem. Commun.*, 2010, **46**, 5289.
- S. N. Georgiades and J. Clardy, *Org. Lett.*, 2005, **7**, 4091.

